Conformation of the Principal Neutralizing Determinant of Human Immunodeficiency Virus Type 1 in Complex with an Anti-gp120 Virus Neutralizing Antibody Studied by Two-Dimensional Nuclear Magnetic Resonance Difference Spectroscopy†

Anat Zvi, Daniel J. Feigelson, Yehezkiel Hayek, and Jacob Anglister*

Department of Structural Biology, The Weizmann Institute of Science, Rehovot 76100, Israel

Received March 6, 1997; Revised Manuscript Received May 12, 1997⊗

ABSTRACT: The principal neutralizing determinant (PND) of human immunodeficiency virus type 1 (HIV-1) is located in the third hypervariable region (V3) of the virus envelope glycoprotein gp120. The conformation of a V3 peptide of HIV-1_{IIIB} bound to the Fab fragment of an anti-gp120 HIV neutralizing antibody, 0.5β, was studied by ^{1}H NMR spectroscopy. This 18-residue peptide represents the epitope recognized by 0.5β and encompasses most of the PND. The slow off-rate of the peptide prevents the observation of peptide/Fab interactions as well as intramolecular interactions within the bound peptide by transferred nuclear Overhauser enhancement (TRNOE). To detect and assign interactions within the bound peptide in the 52 kDa complex, NOESY difference spectra were measured using three strategies: (a) deuteration of peptide residues, (b) Arg → Lys replacements, and (c) truncation of the peptide antigen. Each difference spectrum was calculated between NOESY spectra measured for two Fab complexes in which the bound peptides differed in their deuteration or in their sequence. The difference spectra revealed numerous interactions between the N-terminus of the epitope (Arg-4, Lys-5, Ser-6, Ile-7, and Ile-9) and its C-terminus (Phe-17, Val-18, Thr-19, and Ile-20). The assigned NOE interactions within the bound peptide were translated into distance restraints that were used to calculate the conformation of the bound peptide by the hybrid distance geometry/simulated annealing method. A total of 39 long-range (residues $i - j > 4$), 14 short-range, and 69 intraresidue NOE interactions within the bound peptide have been assigned. Twelve structures without NOE constraint violations were obtained, having a 1.6 Å rms deviation for the backbone atoms. The peptide forms a 10-residue loop, while the two segments flanking this loop, KSI and VTI, interact extensively with each other and possibly form antiparallel β-strands. This loop conformation could be observed due to the unusual large size (17 residues) of the antigenic determinant recognized by 0.5β.

The HIV-1[1] envelope glycoproteins, gp120 and gp41, are targets for virus-neutralizing antibodies. A major fraction of these antibodies in infected individuals or in immunized animals is directed against a determinant located within the third hypervariable region of gp120 (V3 loop). This determinant was designated the principal neutralizing determinant (PND) of the virus and was mapped to a 24 amino acid sequence (NNTRKSIRIQRGPGRAFVTIGKIG), denoted RP135 (residues 308−331 of gp120) (Javaherian et al., 1990; Matsushita et al., 1988). Antibody binding to V3 or V3 deletion does not prevent the virus binding to CD4, which is the primary receptor of the virus. Still, they do prevent virus fusion with its target cells, thus abolishing the virus infectivity (Skinner et al., 1988).

Neutralization of a variety of HIV-1 field isolates has been shown with serum obtained after immunization with antigens containing V3 peptides of different strains (Honda et al., 1995; Hamajima et al., 1995). Anti-HIV-1 human monoclonal antibodies directed against V3 that are capable of neutralizing primary isolates have been obtained as well (Conley et al., 1994). Phase I clinical trials of candidate vaccines containing V3 peptides are being conducted (Rubinstein et al., 1994; Gorse et al., 1996; Salmon-Céron et al., 1995). Immunization with a "cocktail" of peptides may overcome the variability of V3.

The V3 sequence also determines the virus phenotype and the type of cell it will infect (macrophages or T-cells). The basis of the cellular tropism and the role of V3 in viral fusion and in determining the virus phenotype was recently clarified by the identification of second receptors for gp120: fusin

† This work was supported by the Israel Science Foundation, a Philip Feinberg Memorial Research grant in AIDS-related research—a collaborative project between the Weizmann Institute and the American Foundation for AIDS Research—and by the Helen and Milton Kimmelman Center for Biomolecular Structure at the Weizmann Institute.

* To whom correspondence should be addressed.

⊗ Abstract published in *Advance ACS Abstracts,* July 1, 1997.

[1] Abbreviations: CD4, a protein found on the membrane of helper T-cells, macrophages, and monocytes; Fab, antibody fragment made of the Fv and one constant region of both the light and heavy chains; Fv, antibody fragment made of the variable regions of the light and heavy chains; gp120 and gp140, envelope glycoproteins of HIV-1; HIV, human immunodeficiency virus; HOHAHA, homonuclear Hartmann−Hahn two-dimensional experiment; NOE, nuclear Overhauser enhancement; NOESY, two-dimensional nuclear Overhauser enhancement spectroscopy; PBS, phosphate-buffered saline; PND, principal neutralizing determinant; rms, root mean square; RP135, a peptide (NNTRKSIRIQRGPGRAFVTIGKIG) corresponding to the PND of gp120 of the HIV-1_{IIIB} strain; TRNOE, transferred nuclear Overhauser enhancement; $T_{1\rho}$, relaxation time in the rotating frame; T_2, transverse relaxation time; 1D and 2D, one- and two-dimensional. Throughout this paper, the numbering of the residues in the different peptides is according to the sequence of RP135 (NNTRKSIRIQRGPGRAFVTIGKIG).

S0006-2960(97)00520-5 CCC: $14.00

in T-cells (Feng et al., 1996) and CC-CKR-5 in macrophages (Dragic et al., 1996; Deng et al., 1996; Choe et al., 1996; Alkhatib et al., 1996; Doranz et al., 1996). Human anti-V3 antibodies (447-D, 83.1, 19b, and Loop2) were found to inhibit the binding of CC-CKR-5 to gp120 from a macrophage-tropic strain, after the initial binding of CD4 to gp120 (Wu et al., 1996; Trkola et al., 1996). This could be explained either if relatively conserved determinants in V3 are involved in the binding to CC-CKR-5 or if V3 is proximal to the gp120 binding site for CC-CKR-5 and neutralizing antibodies mask this site upon binding to V3 (Wu et al., 1996; Trkola et al., 1996).

The antibody 0.5β (Matsushita et al., 1988) was raised against gp120 of the HIV-1_{IIIB} strain purified from infected cells. The 0.5β antibody was found to protect chimpanzees from HIV infection by passive immunization when administered as a chimeric antibody that contains the intact variable regions of 0.5β and the human constant regions (Emini et al., 1992). The antibody binds gp120 and the 24-residue V3 peptide RP135 with a similar affinity (binding constants of 2×10^8 M^{-1} and 7×10^7 M^{-1}, respectively; Skinner et al., 1988).

A better insight into HIV neutralization would be achieved by studying the interactions of neutralizing antibodies with the PND and by elucidating the structure of the antibody-bound V3 loop at the molecular level. To date, the crystal structure of two complexes of antipeptide HIV neutralizing antibodies in complex with synthetic peptides derived from the V3 loop of the HIV-1_{MN} strain have been determined by Wilson and co-workers (Rini et al., 1993; Ghiara et al., 1994). These antipeptide antibodies recognize small overlapping epitopes (seven residues each with an overlap of three residues). However, there is no structural information on anti-gp120 HIV neutralizing antibodies and their complexes with either gp120 or PND peptides.

NMR studies of the conformation of ligands bound to large proteins (>40 kDa) have been carried out mostly using TRNOE, which requires a fast ligand off-rate (Clore et al., 1986; Behling et al., 1988; Scherf et al., 1992; Ni et al., 1992; Sykes, 1993). Isotope-edited experiments using ^{13}C and ^{15}N labeling of either the ligand or the protein allow studies of tightly bound ligands (Fesik et al., 1988). These experiments were applied to determine the conformation of ligands in complexes smaller than 35 kDa (Fesik et al., 1991; Weber et al., 1991; Ikura et al., 1992). For larger proteins, the signal-to-noise ratio in these experiments is poor due to shorter ^{13}C and ^{15}N T_2 relaxation times. Despite this problem, Wright and co-workers successfully applied isotope-edited experiments to study some features of the secondary structure of ^{15}N- and ^{13}C-labeled peptide bound to a Fab fragment (Tsang et al., 1992).

Difference spectroscopy using a deuterated three-residue peptide inhibitor of pepsin was applied by Fesik et al. (1989) to study the conformation of the inhibitor bound to pepsin. We have recently used this approach in our studies of the 0.5β complex with a 16-residue peptide of the V3 loop of HIV-1_{IIIB} (Zvi et al., 1995b). Most of the peptide residues were specifically deuterated, and the difference spectra between the complex with the deuterated peptide and the complex with the unlabeled peptide revealed a number of intramolecular NOE interactions observed between the N- and C-terminal residues of the peptide. These interactions were indicative of a loop formed by the peptide when bound to the anti-gp120 HIV neutralizing antibody. The limited number of observed NOE interactions was not sufficient to calculate the structure of the bound peptide. In the current study, we used three strategies to calculate NOESY difference spectra: (a) deuteration of peptide residues, which includes specific deuteration of Thr-19 and deuteration of all residues of the peptide excluding arginines, lysine, serine, and threonine; (b) replacement of arginine residues by lysine; and (c) truncation of RP135 at different positions. From the NOESY difference spectra measured for Fab complexes with peptides differing in their deuteration or in their sequence we obtained a large number of long-range distance constraints that enabled us to calculate the structure of the peptide when bound to 0.5β Fab.

MATERIALS AND METHODS

Peptides and Antibody Synthesis and Purification. The different peptides were synthesized using an automated peptide synthesizer and purified by gel-filtration chromatography followed by HPLC, as previously described (Zvi et al., 1995a). Perdeuterated L-amino acids (isoleucine, glutamine, glycine, proline, alanine, valine, and threonine) and L-phenyl-d_5-alanine, with minimum isotopic purity of 98% ^2H were obtained from MSD Isotopes, Canada. The deuterated amino acids (except threonine) were protected with the *t*-butyloxycarbonyl group (t-Boc) and purified by Oz Chemicals, Israel. Threonine was protected with the 9-fluorenylmethyloxycarbonyl group (f-Moc). The preparation and purification of the antibody and its cleavage to the Fab fragment were described elsewhere (Zvi et al., 1995a).

NMR Sample Preparation. The two samples used for each difference spectrum measurement were prepared from the same batch of Fab cleavage, contained the same concentration of Fab/peptide complex, and were treated in the same manner. First, the Fab was dialyzed extensively against D_2O and then the lyophilized peptide was added in an excess of 20−50% to ensure saturation of the Fab. To remove any excess of peptide, the complex was further subjected to dialysis against 10 mM phosphate-buffered D_2O, pH 7.0, containing 0.05% NaN_3. The concentration of the complex for all difference spectra was 1.0−1.6 mM.

NMR Measurements. All NMR spectra were measured on AM500 and DMX500 Bruker spectrometers in the phase-sensitive mode using the time-proportional phase incrementation method (Marion et al., 1983). Each of the two NOESY spectra used in the difference spectrum calculation was measured consecutively at identical experimental conditions and parameters. All measurements were done at 42 °C. The carrier frequency was set on the HDO signal. The residual water signal was suppressed by presaturation during a relaxation delay of 2.3−3.0 s. The mixing time was set to 70 ms. Possible effects of spin diffusion were excluded by comparing the measurements to spectra recorded with 40 ms (Zvi et al., 1995b). A total of 2K data points was collected in the F_2 dimension with a spectral width of 7000 Hz and 146.2 ms acquisition time. In the F_1 dimension, 256 points were measured, with 80−96 scans for each increment of t_1. The acquisition time in the F_1 dimension was 18.3 ms. The sampling delay was set to $d0 = [IN0/2]-[2PW/\pi]$, wherein INO is the dwell time in the F_1 dimension and PW is the length of the 90° pulse, to ensure a zero- and first-order phase corrections of 90° and −180°, respectively,

in the F_1 dimension and a minimal baseline distortion (Bax et al., 1991). All spectra were calibrated versus 3-(trimethylsilyl)propionic-*2,2,3,3-d*$_4$ acid (sodium salt). The data were processed using Bruker's UXNMR software. A zero-filling in the F_1 dimension and a square sine-bell window shifted by 60° in both dimensions were applied prior to two-dimensional Fourier transformation. A further phase correction was applied in F_2 when needed. The procedure for subtraction of the spectra was described previously (Zvi et al., 1995b).

ELISA Binding Measurements. Competitive enzyme-linked immunosorbent assay (ELISA) was employed to determine the affinity of the antibody to the R8H and R15K mutants of RP135 (NNTRKSIRIGPGRAFVTIGKIG) and to the R4K, R8K, and R11K mutants of RP135a (RKSIRIGPGKAFVT) (the numbering of the residues in all peptides is according to the sequence of RP135). All ELISA measurements were conducted following a procedure described by Baillou et al. (1993). Plates were read on a Dynatech MR500 ELISA reader with a 620 nm filter. Affinity constants were determined by Scatchard analysis (Friguet et al., 1985; Stevens 1987).

Structure Calculations. All calculations were carried out on a Silicon Graphics workstation, using the program XPLOR (Brünger, 1992). A total of 53 interresidue constraints and 69 intraresidue constraints were obtained from the NOESY difference spectra. For protons that were not stereospecifically assigned, the distance constraints were averaged according to R^{-6} (Brünger et al., 1986; Levy et al., 1989; Constantine et al., 1992). A correction of 0.5 Å was added to the upper bound of constraints involving a methyl group and 1 Å in case of a methyl−methyl interaction. The constraints were then classified into strong (1.8−2.5 Å), medium (1.8−3.5 Å), and weak (1.8−4.5 Å) and subjected to hybrid distance geometry−dynamical simulated annealing calculations (Nilges et al., 1988). In this method, substructures comprising only a subset of atoms are generated by metric matrix distance geometry. These substructures are then used as a starting point for the dynamical simulated annealing calculations. The total target function in the dynamics calculation for which the global region is searched represents the effective potential energy and comprises a covalent term, a repulsion term, and a term for the NOE distance restraints.

RESULTS

NOESY Difference Spectra Using a Specifically Deuterated Peptide. In the current experiment, we used the peptide RKSIRIQRGPGRAFVTI comprising the full epitope recognized by 0.5β, including Ile-20, which was truncated in our previous study (Zvi et al., 1995b). The aliphatic region of the difference spectrum between the NOESY spectrum of the Fab complex with the unlabeled peptide and the NOESY spectrum of the Fab complex with a peptide specifically deuterated at Thr-19 is shown in Figure 1. This spectrum shows with a remarkable signal-to-noise ratio intraresidue interactions of the labeled residue and interresidue interactions between the specifically labeled residue and protons of the peptide or the Fab. All other cross peaks of the 52 kDa complex are practically canceled out by the subtraction. As revealed from this spectrum, the interactions of Thr-19 are crucial for elucidating the conformation of the

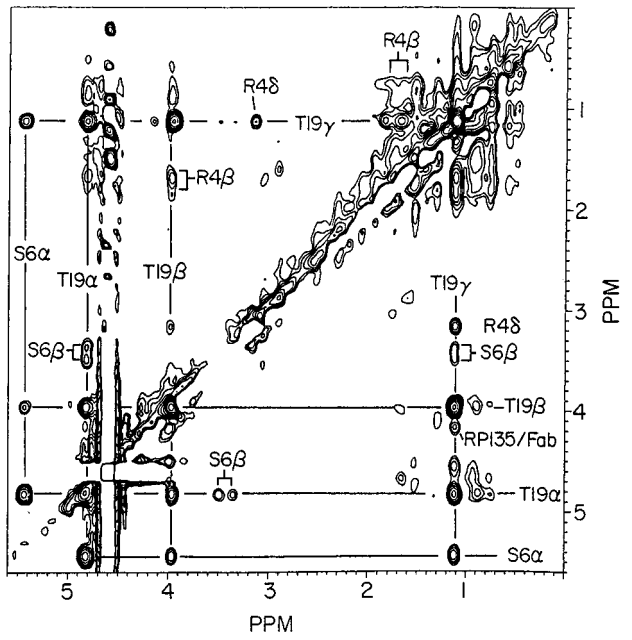

FIGURE 1: Aliphatic region of the difference spectrum between the NOESY of the Fab complex with the unlabeled peptide (RKSIRIQRGPGRAFVTI) and the NOESY of the Fab complex with the peptide in which Thr-19 was specifically deuterated; the numbering of the residues is according to the sequence of RP135 (NNTRKSIRIQRGPGRAFVTIGKIG).

bound peptide. Very strong cross peaks between Thr-19 and Ser-6 backbone and side-chain protons indicate that these two residues are in close contact. (The numbering of the residues in all peptides is according to the sequence of RP135, NNTRKSIRIQRGPGRAFVTIGKIG.) Long-range interactions are also observed between Thr-19 and Arg-4 (the assignment of Arg-4 and Ser-6 protons is based on experiments discussed below). Thr-19 $C_\alpha H$, $C_\beta H$, and $C_\gamma H$ interact with an aromatic proton of Phe-17 (data not shown). It should be noted that no cross peaks between protons of Thr-19 and aromatic protons of the Fab were detected. The interactions observed in Figure 1 add to the extensive network of interactions already found between the N-terminus (Ile-7 and Ile-9) and the C-terminus (Val-18) of the peptide (Zvi et al., 1995b).

NOESY Difference Spectra Using a Deuterated Peptide. As mentioned above, the specific deuterations described previously (Zvi et al., 1995b) were conducted on a peptide lacking Ile-20. Considering that the full epitope recognized by the antibody includes Ile-20, and in view of the numerous NOEs between the N-terminus and the C-terminus of the peptide, Ile-20 may be involved in these intrapeptide interactions as well. To study the interactions in the complete epitope while avoiding the repetition of the measurements using specific deuterations, we used the peptide RK**SIRIQ**R**GPG**R**AFVTI**G (RP135b) in which Ile-7, Ile-9, Gln-10, Gly-12, Pro-13, Gly-14, Ala-16, Phe-17, Val-18, and Ile-20 were deuterated (the deuterated residues are in boldface type). Figure 2 shows the difference between the 1D spectrum of the 0.5β Fab complex with unlabeled RP135b and the spectrum of the complex with the deuterated peptide. This difference spectrum shows the resonances of the deuterated residues with a remarkable signal-to-noise ratio and is used to distinguish between NOESY cross peaks due to interactions within the bound peptide and NOESY cross peaks due to peptide/Fab interactions. The assignment of

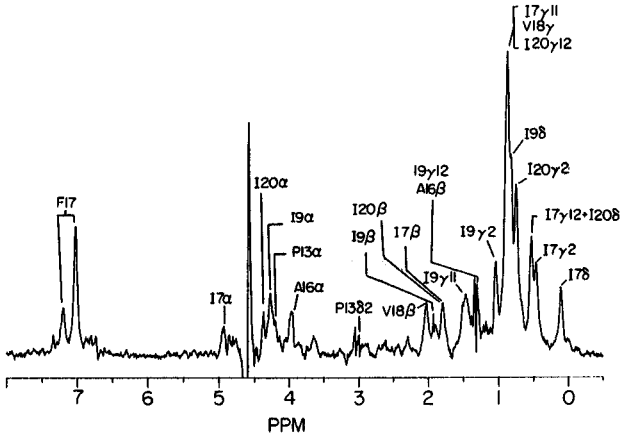

FIGURE 2: Difference between the 1D spectrum of 0.5β Fab complex with RP135b (RKSIRIQRGPGRAFVTIG) and the spectrum of the Fab complex with a peptide molecule in which Ile-7, Ile-9, Gln-10, Gly-12, Pro-13, Gly-14, Ala-16, Phe-17, Val-18, and Ile-20 were deuterated.

the peptide resonances in the 1D difference spectrum is based on the specific deuterations of the individual residues (Zvi et al., 1995b). Panels A and B of Figure 3 show the aromatic and aliphatic regions of the 2D NOESY difference spectrum calculated from the NOESY spectra of the above complexes, respectively. Along with the interactions that were previously observed with the peptide lacking Ile-20 and Gly-21 (Zvi et al., 1995b), the NOESY difference spectrum in Figure 3B shows the interactions of an additional spin system that was assigned to Ile-20 according to the pattern of intraresidue NOE connectivities (this assignment was further confirmed by a difference spectrum calculated with a peptide specifically labeled at Ile-20). Interresidue interactions between Ile-20 and Lys-5 and between Ile-20 and Ile-7 appear in the spectrum. In contrast to the strong NOE cross peaks observed for Ile-7, Ile-9, Ala-16, Phe-17, Val-18, and Ile-20, only weak cross peaks were observed for Gln-10 and Pro-13 and the resonances of neither of the glycines could be assigned at all at this stage. In the aromatic region of the difference spectrum (Figure 3A), we observed the interactions of the aromatic protons of the peptide's Phe-17 with Ser-6, Ile-7, and Thr-19. The assignment of the interactions to Lys-5 and Ser-6 is based on experiments using truncated peptides and will be explained below. The assignment of Thr-19 was done according to Figure 1. In addition to the intramolecular interactions of Phe-17 aromatic protons, Figure 3A reveals several intermolecular NOEs between the aromatic protons of the Fab and Ile-7, Ile-9, Pro-13, Phe-17, and Ile-20 of the peptide.

NOESY Difference Spectra Using Arg → Lys Replacements. The peptide RP135 contains four arginine residues, which were not deuterated for any of our experiments. To save the costs of using deuterated arginine, we introduced conservative replacements of these four residues. A similar approach was used in our studies of the anti-cholera toxin peptide antibody TE34 by TRNOE difference spectroscopy (Anglister & Zilber, 1990). To assess the influence of the replacements on the binding to the antibody, we measured the affinity of each of the five modified peptides (R4K, R8K, R8H, R11K, and R15K) to the antibody by competitive ELISA binding measurements. While the binding of the peptides with R4K and R11K replacements is comparable to that of the unmodified peptide, the mutations R8K, R8H, and R15K reduce the binding by more than 2 orders of magnitude (the mutation R8H was introduced to exclude the possibility that the reduction in binding of R8K was due to the β-breaking character of lysine in comparison with arginine; in this respect, histidine is a conservative mutation). In view of these results, only two of the five modified peptides were used in NOESY difference spectra measurements. The 1D difference spectra calculated for the R4K and for the R11K replacements contain almost solely the positive and negative resonances attributed to arginine and lysine, respectively (data not shown). However, the NOESY difference spectra contain not only cross peaks assigned to arginine (positive) and lysine (negative) but also some cross peaks that arise from local changes in the relative disposition of residues that occur both in the Fab and in the peptide as a result of the replacements. For example, the NOESY difference spectrum calculated for the R11K replacement shows also the resonances of Gln-10 (Figure 4). A system of cross peaks between resonances at 2.37, 2.73, and 4.88 is typical of an AMX system and has not been assigned to any peptide protons. This system of cross peaks, which is accompanied by negative cross peaks of the Fab complex with the modified peptide, could be due to intraresidue cross peaks of the Fab. Examination of the part of the NOESY spectrum showing aromatic proton interactions reveals no cross peaks between the nonlabile protons of Arg-4 and Arg-11 and the aromatic protons of the Fab.

NOESY Difference Spectra Using Truncated Peptides. We used truncated peptides to study the interactions of residues that were neither deuterated nor replaced (Lys-5, Ser-6, Arg-8, and Arg-15). The difference between the spectrum of the Fab complex with the peptide **NNTR**KSIRIQRGPGRAFVTI and the spectrum of the Fab complex with the peptide KSIRIQRGPGRAFVTI is shown in Figure 5. In addition to the cross peaks of Thr-3 and Arg-4 that were truncated in the second peptide, this difference spectrum shows the cross peaks of Lys-5, which became the N-terminal residue, and the cross peaks of Ser-6, Thr-19, and Ile-20. Thr-3 was assigned on the basis of the HOHAHA spectrum of the 0.5β Fab/RP135 complex. (The $T_{1\rho}$ of residues that are outside the epitope, namely, Asn-1, Asn-2, Thr-3, Gly-21, Lys-22, Ile-23, and Gly-24, is considerably longer than that of the Fab protons, and therefore they can be detected by the HOHAHA experiment with a good signal-to-noise ratio despite the molecular weight of the complex; Zvi et al., 1995a.) Lys-5 was assigned on the basis of the typical cross-peak pattern of its spin system. The cross peaks of Ser-6 appear due to its proximity to the N-terminus of the truncated peptide. Its assignment was based on the typical spin system and was further verified by another difference spectrum (see below). Thr-19 and Ile-20 were previously assigned (Figures 1 and 3B, respectively). Strong interactions are again observed between Arg-4 and Thr-19, between Ser-6 and Thr-19, and between Lys-5 and Ile-20. The interactions of Thr-19 (excluding the Thr-19/Arg-4 interaction) and the interactions of Ile-20 appear as both positive and negative cross peaks as both peptides contain these residues. The truncation of the four N-terminal residues of RP135 induces small but still observable changes in the chemical shifts of residues at the C-terminus of the determinant recognized by the antibody (Thr-19 and Ile-20) due to the long-range interactions between the N- and C-termini of the epitope.

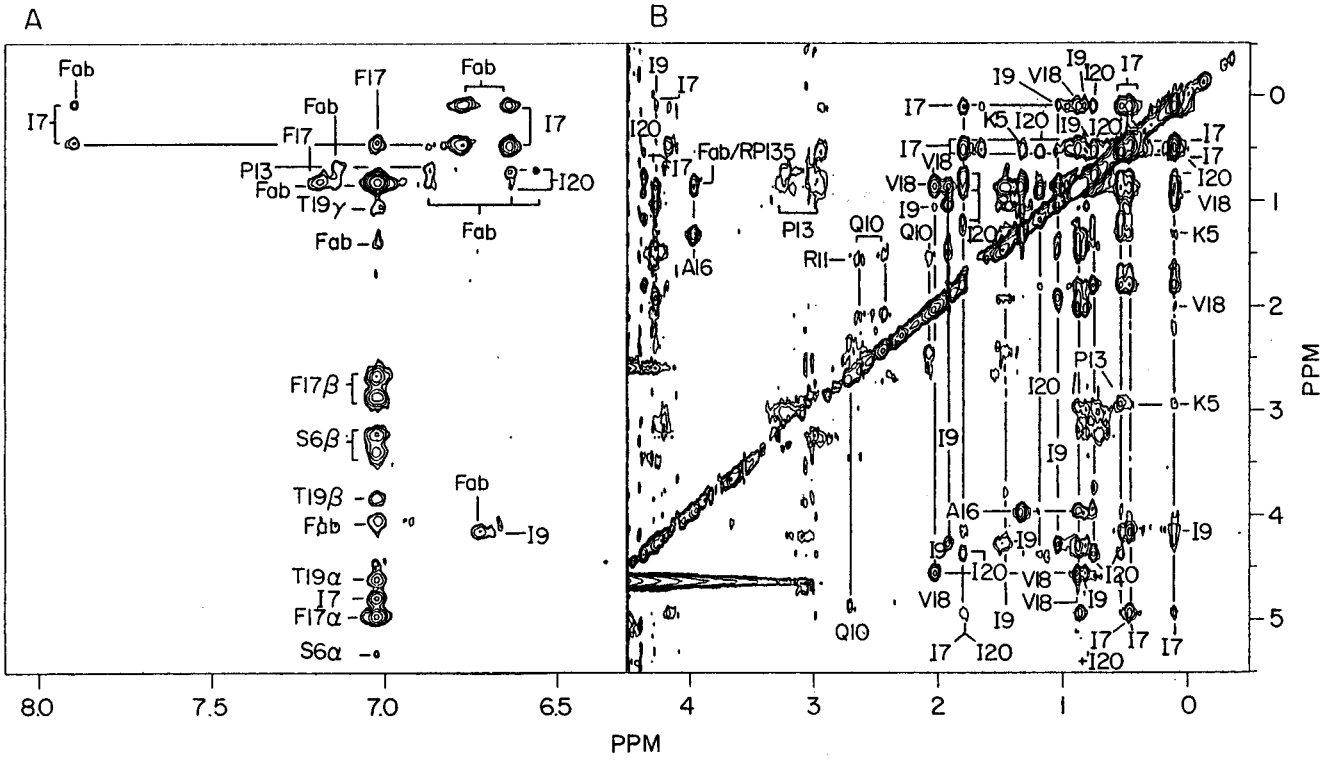

FIGURE 3: Difference between the NOESY spectrum of 0.5β Fab complex with the peptide RP135b (RKSIRIQRGPGRAFVTIG) and the spectrum of the Fab complex with a peptide molecule in which Ile-7, Ile-9, Gln-10, Gly-12, Pro-13, Gly-14, Ala-16, Phe-17, Val-18, and Ile-20 were deuterated. The assignments of the cross peaks are marked for the F_1 and the F_2 dimensions: (A) a section of the difference spectrum, showing the interactions of aromatic protons of 0.5β Fab and Phe-17 of the peptide with nonaromatic protons of the peptide and (B) the aliphatic section of the difference spectrum.

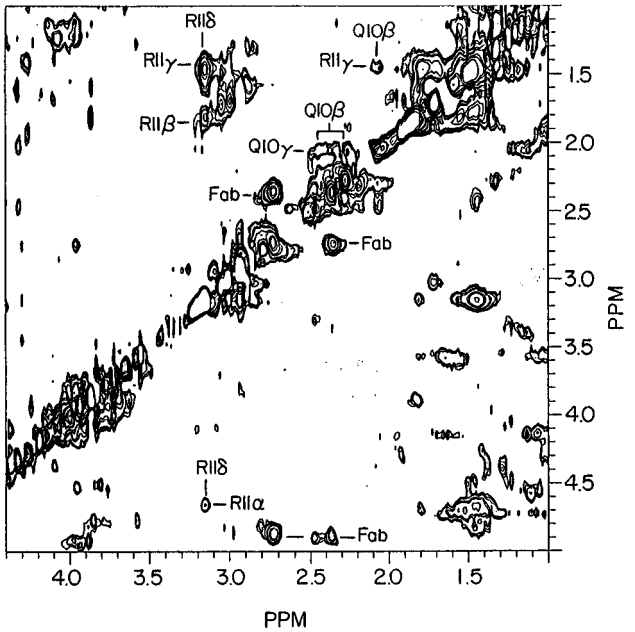

FIGURE 4: Difference between the NOESY spectrum of 0.5β Fab complex with the peptide RP135a (RKSIRIQRGPGRAFVT) and the spectrum of the Fab complex with a peptide molecule in which Arg-11 was replaced by Lys. Only positive cross peaks arising from the Fab complex with the unmodified peptide are shown.

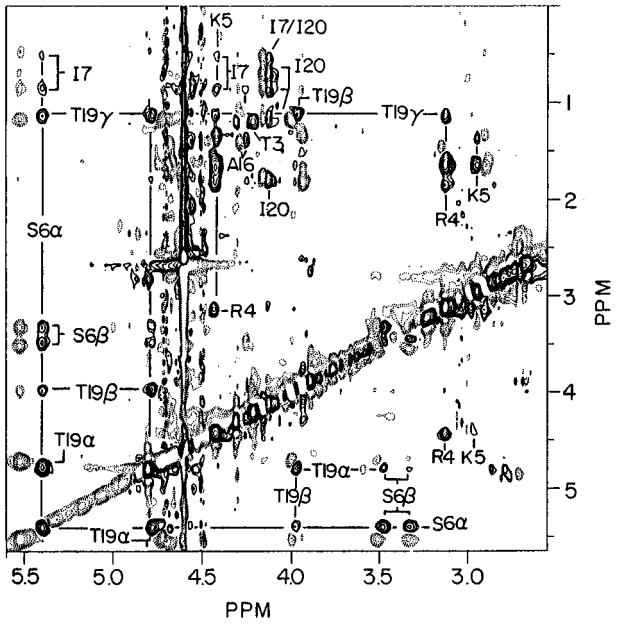

FIGURE 5: Section of the difference between the NOESY spectrum of 0.5β Fab complex with the peptide **NNTR**KSIRIQRGPGRAFVTI (the residues missing in the second peptide are in boldface type) and the complex with the peptide KSIRIQRGPGRAFVTI. Solid line, positive phase of the spectrum showing cross peaks arising from the first complex; dotted line, negative phase of the spectrum, contributed by the second complex.

To verify the assignment of Ser-6 cross peaks, we calculated the difference spectrum of the Fab complex with the peptide SIRIQRGPGRAFVTIGKIGKGKK and the Fab complex with a peptide having the same sequence but with the serine N-acetylated (**Ac-SIRIQRGPGRAFVTIGK-IGKGKK**). The acetylation of the N-terminal amine of the peptide abolishes its positive charge and therefore is expected to considerably affect the chemical shift of $C_\alpha H$ of Ser-6. Otherwise, the differences between the two complexes should be rather minor. Indeed, as shown in Figure 6, the positive cross peaks at 5.15 ppm assigned to $C_\alpha H$ of Ser-6 are no longer accompanied by negative cross peaks with similar

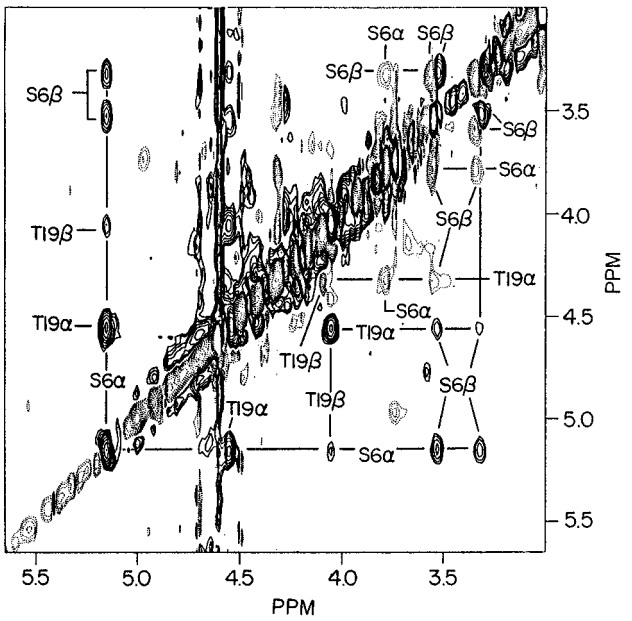

FIGURE 6: Difference between the NOESY spectrum of the 0.5β Fab complex with the peptide N-acetyl-SIRIQRGPGRAFVTIGKIG-GKK and the complex with the peptide SIRIQRGPGRAFVTIGKIG-GKK. Solid line, positive phase of the spectrum, showing cross peaks of residues from the acetylated peptide; dotted line, negative phase contributed by the complex with the nonacetylated peptide.

Table 1: Interresidue Interactions within the Bound Peptide

Arg-4	Thr-19
Lys-5	Ile-7, Ile-20
Ser-6	Ile-7, Phe-17, Thr-19
Ile-7	Lys-5, Ser-6, Ile-9, Phe-17, Val-18, Ile-20
Ile-9	Ile-7, Val-18
Gln-10	Arg-11
Arg-11	Gln-10
Phe-17	Ser-6, Ile-7, Thr-19
Val-18	Ile-7, Ile-9
Thr-19	Arg-4, Ser-6, Phe-17
Ile-20	Lys-5, Ile-7

(but not identical) chemical shifts. On the other hand, the positive cross peaks between the C_β protons of Ser-6 in the acetylated peptide are still accompanied by negative cross peaks with similar chemical shifts in the nonacetylated peptide. The pattern of the negative cross peaks between the resonances at 3.32, 3.60, and 3.80 is typical of serine and therefore the resonance at 3.8 is assigned to Ser-6 $C_\alpha H$ of the nonacetylated peptide. The C_α proton undergoes an upfield change of 1.35 ppm upon acetylation of the N-terminus, and its chemical shift resembles that of the $C_\alpha H$ of Ser-6 in the RP135 peptide (see Figure 4). Table 1 summarizes the intramolecular interactions observed in the bound peptide.

Model of the Bound Peptide. A total of 122 distance restraints were derived from the NOE cross peaks that were assigned to interactions within the bound peptide. They consist of 39 long-range ($i-j > 4$ residues), 14 short-range, and 69 intraresidue distance restraints. No long-range restraints were obtained for Arg-8 and for residues 10−16. The NOE-derived distance restraints were used in hybrid distance geometry/simulated annealing calculations (Nilges, 1988) to obtain the conformation of the bound peptide (RKSIRIQRGPGRAFVTI), which is shown in Figure 7. A total of 12 refined structures with no NOE violations greater than 0.5 Å were calculated. The rms deviation between the

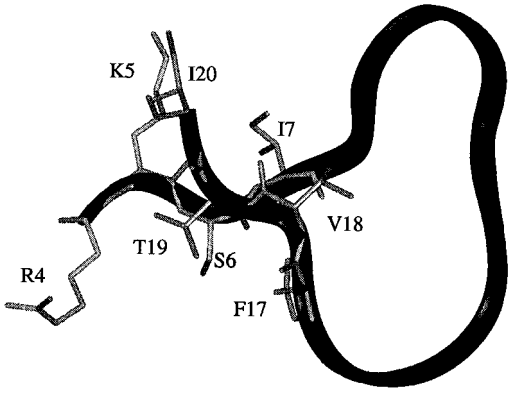

FIGURE 7: Mean structure of the 12 best-fit lowest energy calculated models for the peptide conformation when bound to 0.5β Fab. The mean structure was subjected to a short run of energy minimization; the peptide backbone is shown in a ribbon style, and side chains of interacting residues are shown as sticks. The figure was generated using the program Insight II (Biosym/MSI).

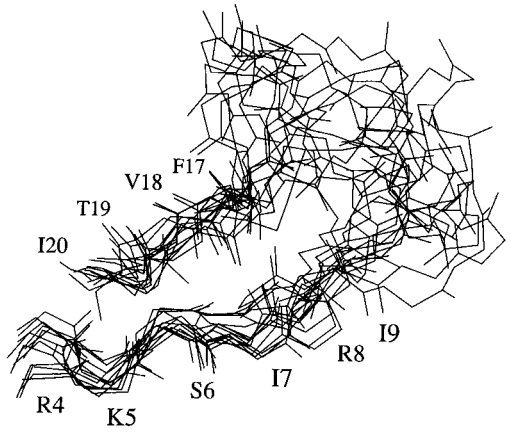

FIGURE 8: Superposition of the 12 lowest energy calculated models for the peptide conformation when bound to 0.5β Fab. Only backbone atoms are shown. The fit was optimized for the backbone of residues 4−9 and 17−20. The structures were superimposed on the mean structure, which was first subjected to a short run of energy minimization.

individual structures and the energy-minimized average structure is 1.1 Å for backbone atoms of residues 5−9 and 17−20. The backbone and all-atoms rms deviations for all 17 residues of the peptide are 1.6 and 2.7 Å, respectively. The superposition of the 12 best-fit lowest energy structures on the mean structure is shown in Figure 8. The fit was optimized for the backbone of residues 4−9 and 17−20. For Ser-6, Ile-7, Ile-9, Phe-17, Val-18, Thr-19, and Ile-20, we obtained an average of 10 long-range constraints/residue. The peptide forms a 10-residue loop (residues 8−17), while the two segments flanking this loop from opposite sides, KSI (5−7) and FVTI (17−20), interact extensively with each other. Most of the residues in these two segments are in an extended conformation and possibly form antiparallel β-strands, thus creating a β-hairpin. A very strong interaction between $C_\alpha H$ of Ser-6 and $C_\alpha H$ of Thr-19 [$d_{\alpha,\alpha}$ (i, j)] is indeed indicative of antiparallel β-strands. Lys-5, Ile-7, Ile-9, Val-18, and Ile-20 side chains point to one side of the β-structure while the side chains of Arg-4, Ser-6, Phe-17, and Thr-19 are on the other side. This is concluded from the strong interactions that appear between alternating residues: Lys-5 and Ile-7 side chains interact with Ile-20, and the side chains of both Ile-7 and Ile-9 interact with the side chain of Val-18, forming a mainly hydrophobic surface. Arg-4 interacts

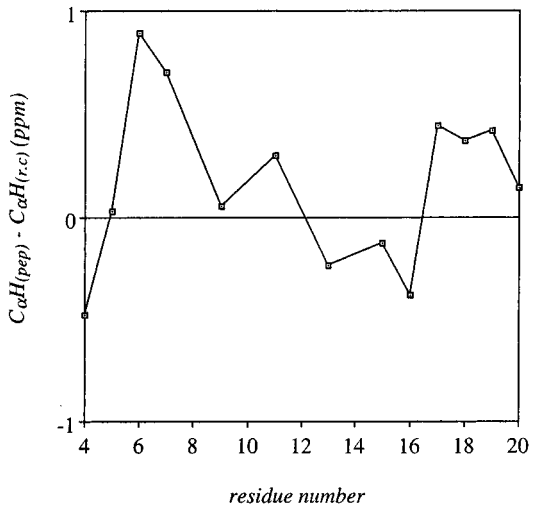

FIGURE 9: Deviation of the $C_\alpha H$ chemical shifts from their random coil values as a function of the residue number.

with Thr-19, and Ser-6 interacts with Phe-17 and Thr-19. The side chains of these four residues form a mostly polar surface. Another evidence supporting the proposed antiparallel β-sheet structure is the deviations from random coil values of the $C_\alpha H$ chemical shifts. The $C_\alpha H$ chemical shift of residues in a β conformation are expected to experience downfield deviation in comparison to their random coil values (Williamson et al., 1990). Figure 9 shows the changes in the chemical shifts of the C_α protons per residue. Positive values are indeed observed for residues SI and FVTI. Due to lack of constraints, the conformation of the seven-residue segment QRGPGRA is poorly defined.

DISCUSSION

In the present study, ^{1}H NOESY difference spectroscopy was used to study the bound peptide conformation in complex with the Fab, employing three strategies: (a) deuteration of peptide residues, (b) Arg → Lys replacements, and (c) truncation of the peptide antigen. The difference spectra measured using deuterated residues are the simplest and easiest to interpret. Difference spectra using truncated or modified peptides are usually more complicated. However, these last two types of spectra contain mainly the contribution of the truncated or modified residues if the modification is only minor and does not alter the binding considerably: for example, the difference spectrum measured using the peptide SIRIQRGPGRAFVTIGKIGGKK and its N-terminal-acetylated form and the difference spectrum measured using the peptides NNTRKSIRIQRGPGRAFVTI and KSIRIQRGPGRAFVTI. In the latter case, Arg-4, which is at the N-terminus of the epitope, is truncated. This modification does not cause any significant change in the binding constant of 0.5β to the peptide antigen. However, the difference spectrum calculated using RP135 and the peptide RKSIRIQRGPGRAFVT (data not shown) resulted in a complicated difference spectrum as the truncation of Ile-20, which is at the C-terminus of the epitope, caused a 2 orders of magnitude decrease in the binding constant. Since Ile-20 interacts with Lys-5 and Ile-7 at the N-terminal part of the peptide, upon its truncation these residues experienced changes in their proton chemical shifts.

The three types of difference spectra that have been presented use the sensitivity of the ^{1}H NOESY spectrum and do not rely on coherence transfer as the isotope-edited experiments using ^{13}C or ^{15}N labeled ligands do. The coherence transfer steps in the isotope-edited measurements reduce considerably the signal-to-noise ratio in spectra of large proteins (> 40 kDa) due to the decreasing transverse relaxation times.

The NOE constraints derived from the NOESY difference spectra enabled us to calculate the conformation of the peptide representing the PND of the HIV when it is bound to the Fab fragment of an HIV-neutralizing antibody. The conformation of peptides bound to proteins of comparable size has been determined so far only by TRNOE methods (Sykes et al., 1993). Complexes of proteins larger than 40 kDa that exhibit tight binding were studied in some details by isotope-editing techniques, using ^{15}N and/or ^{13}C labeling of the peptide; however, the data obtained were not sufficient to calculate the structure of the ligand (Tsang et al., 1992; Derrick et al., 1992).

The loop conformation of the PND peptide was not observed in the free form of the peptide in solution (Zvi et al., 1992), nor was it observed in two complexes of HIV-neutralizing anti-peptide antibodies studied by Wilson and co-workers (Rini et al., 1993; Ghiara et al., 1994). In the free PND peptide, a transient β-turn was observed in the conserved GPGR sequence as well as a nascent helix at the C-terminus of RP135 (Zvi et al., 1992; Chandrasekhar et al., 1991). The PND peptide of the HIV-1_{MN} strain was found to adopt a double-turn conformation in the GPGRAF sequence when it is bound to an HIV-neutralizing anti-peptide antibody (Ghiara et al., 1994). The eight-residue antigenic determinant KRIHIGPG (residues 312−321 in gp120), recognized by 50.1, and the nine-residue antigenic determinant, HIGPGRAFYT (residues 315−326 in gp120), recognized by 59.1, studied by Wilson and co-workers (Rini et al., 1993; Ghiara et al., 1994) were too short to allow the detection of long-range interactions in the PND. In the case of 0.5β, the epitope consists of 17 residues, RKSIRIQRG-PGRAFVTI (residues 311−327 in gp120), thus enabling observations of long-range interactions in the antigenic determinant. It is expected that the conformation of a flexible PND peptide bound to an antibody raised against gp120 is similar to the conformation of the corresponding part of gp120 when bound to the same antibody.

The suggestion that the two regions flanking the GPGR sequence contain segments in a β-strand conformation is also in agreement with the prediction of the secondary structure of the V3 loop (LaRosa et al., 1990; Hansen et al., 1996). According to LaRosa et al. (1990), the segments Ser-6−Gln-10 and Phe-17−Ile-20 form β-strands in the corresponding parts of gp120 of HIV-1_{IIIB}. Of 245 sequences examined by La Rosa et al. (1990), 93% are predicted to have a β strand around positions 6−9, and 49% of the sequences are expected to form a β strand around residue 18 (the numbering of the residues is according to RP135). According to a classification of amino acids as β-sheet favoring, β-sheet indifferent, and β-sheet breaking (Levitt, 1978), none of the 245 sequences examined by La Rosa et al. contains β-sheet breaking residues at positions 18 and 19. Only 5% of the residues at these positions are β-sheet indifferent and the rest are β-sheet favoring. The prediction of La Rosa et al. (1990) and our observations may indicate that the PND conformation that we found is common to most HIV-1 strains.

The β-structure is a highly ordered secondary structure involving a network of hydrogen bonds and side-chain−side-chain interactions. Indeed, numerous interactions between the antiparallel segments KSI and VTI are observed (Table 1). Therefore, it is unlikely that the β-hairpin conformation is induced by the antibody and that this region of gp120 will adopt different structures upon interaction with different antibodies (as could be expected if this region of gp120 was highly flexible). The loop conformation that we present for the PND peptide is also in agreement with a previously predicted structure of the PND of gp120 (Langedijk et al., 1992), calculated on the basis of its sequence similarity to a hairpin loop of REI immunoglobulin (Metlas et al., 1991). The β-structure that we propose for the segments KSIR and FVTI agrees with a recent prediction of the gp120 structure based on neural network and nearest-neighbor algorithms (Hansen et al., 1996). Better definition of the bound peptide conformation may require studies of amide proton interactions and peptide−antibody interactions.

The side chains of Ile-7, Pro-13, Phe-17, and Ile-20 interact with protons of the Fab (Figure 3A), indicating that these peptide residues are exposed in gp120. Their exposure implies that they are amenable to interactions with the coreceptors for gp120 found on T-cells and macrophages (Feng et al., 1996; Dragic et al., 1996) or involved in other processes, as the virus fusion. Ile-7 and Pro-13 of the PND are two of the most conserved residues of V3 among different strains. In view of their conservation, exposure, and interactions with the antibody, it is most probable that these two residues have a crucial functional role in gp120.

ACKNOWLEDGMENT

We are greatly indebted to Dr. Shuzo Matsushita for the 54′CB1 hybridoma cell line producing the 0.5β monoclonal antibody, to Mr. Vitali Tugarinov for his help with XPLOR, to Professor Michael Levitt for most fruitful discussions, to Professor Mati Fridkin and Mrs. Aviva Kapitkovsky for peptide synthesis, and to Mrs. Rina Levy for excellent technical assistance.

SUPPORTING INFORMATION AVAILABLE

A table of the chemical shifts of the bound peptide proton and a list of constraints for the calculation of the model of the bound peptide (8 pages). Ordering information is given on any current masthead page.

REFERENCES

Alkhatib, G., Combadiere, C., Broder, C. C., Feng, Y., Kennedy, P. E., Murphy, P. M., & Berger, E. A. (1996) *Science 272*, 1955−1958.

Anglister, J., & Zilber, B. (1990) *Biochemistry 29*, 921−928.

Baillou, A., Brand, D., Denis, F., M'Boup, S., Chout, R., Goudeau, A., & Barin, F. (1993) *AIDS Res. Hum. Retroviruses 9* (12), 1209−1215.

Bax, A., Ikura, M., Kay, L. E., & Zhu, G. (1991) *J. Magn. Reson. 91*, 174−178.

Behling, R. W., Yamane, T., Navon, G., & Jelinski, L. W. (1988) *Proc. Natl. Acad. Sci. U.S.A. 85*, 6721−6725.

Brünger, A. T. (1992) XPLOR Manual, Yale University, New Haven, CT.

Brünger, A. T., Clore, G. M., Gronenborn, A. M., & Karplus, M. (1986) *Proc. Natl. Acad. Sci. U.S.A. 83*, 3801−3805.

Chandrasekhar, K., Profy, A. T., & Dyson, H. J. (1991) *Biochemistry 30*, 9187−9194.

Choe, H., Farzan, M., Sun, Y., Sullivan, N., Rollins, B., Ponath, P. D., Wu, L., Mackay, C. R., LaRosa, G., Newman, W., Gerard, N., Gerard, C., & Sodrosky, J. (1996) *Cell 85*, 1135−1148.

Clore, G. M., Gronenborn, A. M., Carlson, G., & Meyer, E. F. (1986) *J. Mol. Biol. 190*, 259−267.

Conley, A. J., Gorny, M. K., Kessler, J. A., Boots, L. J., Ossorio-Castro, M., Koenig, S., Lineberger, D. W., Emini, E. A., Williams, C., & Zolla-Pazner, S. (1994) *J. Virol. 68*, 6994−7000.

Constantine, K. L., Madrid, M., Banyai, L., Trexler, M., Patthy, L., & Llinas, M. (1992) *J. Mol. Biol. 223*, 281−298.

Deng, H., Lui, R., Ellmeier, W., Choe, S., Unutmaz, D., Burkhart, M., Marzio, P. D., Marmon, S., Sutton, R. E., Hill, C. M., Davis, C. B., Peiper, S. C., Schall, T. J., Littman, D. R., & Landau, N. R. (1996) *Nature 381*, 661−666.

Derrick, J. P., Lian, L. Y., Roberts, G. C. K., & Shaw, W. V. (1992) *Biochemistry 31*, 8191−8195.

Doranz, B. J., Rucker, J., Yi, Y., Smyth, R. J., Samson, M., Peiper, S. C., Parmentier, M., Collman, R. G., & Doms, R. W. (1996) *Cell 85*, 1149−1158.

Dragic, T., Litwin, F., Allaway, G. P., Martin, S. R., Huang, Y., Nagashima, K. A., Cayanan, C., Maddon, P. J., Koop, R. A., Moore, J. P., & Paxton, W. A. (1996) *Nature 381*, 667−673.

Emini, E. A., Schleif, W. A., Nunberg, J. H., Conley, A. J., Eda, Y., Tokiyoshi, S., Putney, S. D., Matsushita, S., Cobb, K. E., Jett, C. M., Eichberg, J. W., & Murthy, K. K. (1992) *Nature 355*, 728−730.

Feng, Y., Broder, C. C., Kennedy, P. E., & Berger, E. A. (1996) *Science 272*, 872−877.

Fesik, S. W., & Zuiderweg, E. R. P. (1989) *J. Am. Chem. Soc. 111*, 5013−5015.

Fesik, S. W., Luly, J. R., Erickson, J. W., & Abad-Zapatero, C. (1988) *Biochemistry 33*, 3296−3303.

Fesik, S. W., Gampe, R. T., Jr., Eaton, H. L., Gemmecker, G., Olejniczak, E. T., Neri, P., Holzman, T. F., Egan, D. A., Edalji, R., Simmer, R., Helfrich, R., Hochlowski, J., & Jackson, M. (1991) *Biochemistry 30*, 6574−6583.

Friguet, B., Chaffotte, A. F., Djavadi-Ohaniance, L., Goldberg, M. E. (1985) *J. Immunol. Methods 77*, 305−319.

Ghiara, J. B., Stura, E. A., Stanfield, R. L., Profy, A. T., & Wilson, I. A. (1994) *Science 264*, 82−85.

Gorse, G. J., Keefer, M. C., Belshe, R. B., Matthews, T. J., Forrest, B. D., Hsieh, R.-H., Koff, W. C., Hanson, C. V., Dolin, R., Weinhold, K. J., Frey, S. E., Ketter, N., & Fast, P. E. (1996) *J. Infect. Dis. 173*, 330−339.

Hamajima, K., Bukawa, H., Fukushima, J., Kawamoto, S., Kaneko, T., Sekigawa, K. I., Tanaka, S. I., Tsukuda, M., & Okuda, K. (1995) *Clin. Immunol. Immunopathol. 77*, 374−379.

Hansen, J. E., Lund, O., Nielsen, J. O., Brunak, S., & Hansen, J. E. S. (1996) *Proteins: Struct., Funct., Genet. 25*, 1−11.

Honda, M., Matsuo, K., Nakasone, T., Okamoto, Y., Yoshizaki, H., Kitamura, K., Sugiura, W., Watanabe, K., Fukushima, Y., Haga, S., Katsura, Y., Tasaka, H., Komuro, K., Yamada, T., Asano, T., Yamazaki, A., & Yamazaki, S. (1995) *Proc. Natl. Acad. Sci. U.S.A. 92*, 10693−10697.

Ikura, M., & Bax, A. (1992) *J. Am. Chem. Soc. 114*, 2433−2440.

Javaherian, K., Langlois, A. J., LaRosa, G. J., Profy, A. T., Bolognesi, D. P., Herlihy, W. C., Putney, S. D., & Matthews, T. J. (1990) *Science 250*, 1590−1593.

Langedijk, J. P. M., Back, N. K. T., Kinney-Thomas, E., Bruck, C., Francotte, M., Goudsmit, J., & Meleon, R. H. (1992) *Arch. Virol. 126*, 129−146.

La Rosa, G. J., Davide, J. P., Weinhold, K., Waterbury, J. A., Profy, A. T., Lewis, J. A., Langlois, A. J., Dreesman, G. R., Boswell, R. N., Shadduck, P., Holley, L. H., Karplus, M., Bolognesi, D. P., Matthews, T. J., Emini, E. A., & Putney, S. D. (1990) *Science 249*, 932−935.

Levitt, M. (1978) *Biochemistry 17*, 4277−4285.

Levy, R. M., Bassolino, D. A., Kitchen, D. B., & Pardi, A. (1989) *Biochemistry 28*, 9361−9372.

Marion, D., & Wüthrich, K. (1983) *Biochem. Biophys Res. Commun. 113*, 967−974.

Matsushita, S., Robert-Guroff, M., Rusche, J., Koito, A., Hattori, T., Hoshino, H., Javaherian, K., Takatsuki, K., & Putney, S. (1988) *J. Virol. 62*, 2107−2114.

Metlas, R., Veljkovic, V., Paladini, R. D., & Pongor, S. (1991) *Biochem. Biophys. Res. Commun. 179* (2), 1056−1062.
Moore, J. P., & Nara, P. L. (1991) *AIDS 5*, S21−S33.
Ni, F., Ripoll, D. R., Martin, P. D., & Edwards, B. F. P. (1992) *Biochemistry 31*, 11551−11557.
Nilges, M., Clore, M., & Gronenborn, A. (1988) *FEBS Lett. 229*, 317−324.
Rini, J. M., Stanfield, R. L., Stura, E. A., Salinas, P. A., Profy, A. T., & Wilson, I. A. (1993) *Proc. Natl. Acad. Sci. U.S.A. 90*, 6325−6329.
Rubinstein, A., Goldstein, H., Pettoello-Mantovani, M., & Cryz, S. J. (1994) *AIDS Res. Hum. Retroviruses 10*, S149−S153.
Salmon-Céron, D., Excler, J.-L., Sicard, D., Blanche, P., Finkielstzjen, L., Gluckman, J.-C., Autran, B., Matthews, T. J., Meignier, B., Kieny, M.-P., Valentin, C., Gonnet, P., Diaz, I., Salomon, H., Pialoux, G., Gonzalez-Canali, G., & Plotkin, S. (1995) *AIDS Res. Hum. Retroviruses 11*, 1479−1486.
Scherf, T., Hiller, R., Naider, F., Levitt, M., & Anglister, J. (1992) *Biochemistry 31*, 6884−6897.
Skinner, M. A., Ting, R., Langlois, A. J., Weinhold, K. J., Lyerly, H. K., Javaherian, K., & Matthews, T. J. (1988) *AIDS Res. Hum. Retroviruses 4*, 187−197.
Stevens, F. J. (1987) *Mol. Immunol. 24*, 1055−1060.
Sykes, B. D. (1993) *Curr. Opin. Biotechnol. 4*, 392−396.
Trkola, A., Dragic, T., Arthos, J., Binley, J. M., Olson, W. C., Allaway, G. P., Cheng-Mayer, C., Robinson, J., Maddon, P. J., & Moore, J. P. (1996) *Nature 384*, 184−187.
Tsang, P., Rance, M., Fieser, T. M., Ostresh, J. M., Houghten, R. A., Lerner, R. A., & Wright, P. E. (1992) *Biochemistry 31*, 3862−3871.
Weber, C., Wider, G., von Freyberg, B., Traber, R., Braun, W., Widmer, H., & Wuthrich, K. (1991) *Biochemistry 30*, 6563−6574.
Williamson, M. P. (1990) *Biopolymers 29*, 1423−1431.
Wu, L., Gerard, N. P., Wyatt, R., Choe, H., Parolin, C., Ruffing, N., Borsetti, A., Cardoso, A. A., Desjardin, E., Newman, W., Gerard, G., & Sodroski, J. (1996) *Nature 384*, 179−183.
Zvi, A., Hiller, R., & Anglister, J. (1992) *Biochemistry 31*, 6972−6979.
Zvi, A., Kustanovich, I., Feigelson, D., Levy, R., Eisenstein, M., Matsushita, S., Richalet-Secordel, P., Regenmortel, M. H. V., & Anglister, J. (1995a) *Eur. J. Biochem. 229*, 178−187.
Zvi, A., Kustanovich, I, Hayek, Y., Matsushita, S., & Anglister, J. (1995b) *FEBS Lett. 368*, 267−270.

BI970520F